

Modern Physics Letters A
 © World Scientific Publishing Company

SIMULATION OF A COMBINED SZE AND WEAK LENSING CLUSTER SURVEY FOR AMIBA EXPERIMENT

KEIICHI UMETSU

*Institute of Astronomy and Astrophysics, Academia Sinica, P.O. Box 23-141, Taipei 106,
 Taiwan, Republic of China
 keiichi@asiaa.sinica.edu.tw*

TZIHONG CHIUEH, KAI-YANG LIN, JUN-MEIN WU

Department of Physics, National Taiwan University, Taipei 106, Taiwan, Republic of China

YAO-HUAN TSENG

*Institute of Astronomy and Astrophysics, Academia Sinica, P.O. Box 23-141, Taipei 106,
 Taiwan, Republic of China*

Received (Day Month Year)

Revised (Day Month Year)

We present simulations of interferometric Sunyaev-Zel'dovich effect (SZE) and optical weak lensing observations for the forthcoming AMiBA experiment, aiming at searching for high-redshift clusters of galaxies. On the basis of simulated sky maps, we have derived theoretical halo number counts and redshift distributions of selected halo samples for an AMiBA SZE survey and a weak lensing follow-up survey. By utilizing the conditional number counts of weak lensing halos with the faint SZE detection, we show that a combined SZE and weak lensing survey can gain an additional fainter halo sample at a given false positive rate, which cannot be obtained from either survey alone.

Keywords: Cosmology; cosmic microwave background; gravitational lensing; clusters.

PACS Nos.: include PACS Nos.

1. Introduction

The thermal Sunyaev-Zel'dovich effect (SZE¹) is a spectral distortion of the Cosmic Microwave Background (CMB) radiation due to the inverse-Compton scattering of CMB photons by high energy electrons in the intracluster medium (ICM). The most remarkable properties of the SZE is that its surface brightness is redshift independent, which make it as an ideal probe of the high-redshift universe. Further, since the SZE is proportional to the thermal energy content of the ICM, SZE imaging surveys allow us to select clusters over a wide range of the redshift with physically meaningful selection criteria. Weak gravitational lensing, on the other hand, probes the total mass projected along the line-of-sight, and hence provides complementary informa-

tion on the mass of galaxy clusters.² Array for Microwave Background Anisotropy (AMiBA³) is a 19-element interferometric array with full polarization capabilities operating at 95GHz, specifically designed for the CMB observations. One of the main scientific goals of AMiBA is to conduct blind SZE surveys to search for high-redshift clusters. AMiBA will also conduct follow-up optical imaging observations with wide-field camera, MegaCam, at *Canada France Hawaii Telescope* (CFHT). In this paper, we simulate the forthcoming AMiBA SZE experiment combined with the planned follow-up weak lensing observations to examine the expected cluster number counts for individual surveys, and explore the potential of a combined AMiBA SZE and weak lensing cluster survey.

2. Simulation Data and Mock Observations

To make sky maps with realistic SZE and weak lensing signals, we use results from preheating cosmological simulations of a Λ CDM model ($\Omega_m = 0.34, \Omega_\Lambda = 0.66, \Omega_b = 0.044, h = 0.7, \sigma_8 = 0.94$) in a $100h^{-1}$ Mpc co-moving box which reproduce the observed cluster M_X - T_X and L_X - T_X relations at $z = 0$.⁴ We construct 36 SZE sky maps each with 1deg^2 on a 1024^2 grid, by projecting the electron pressure through the randomly displaced and oriented simulation boxes, separated by $100h^{-1}$ Mpc, along a viewing cone out to the redshift of $z = 2$. Similarly, weak lensing convergence (κ) maps are constructed by projecting the distance-weighted mass over-density $\delta\rho$ out to a source plane at $z = z_s$.

As an AMiBA specification, we adopt a close-packed hexagonal configuration of $19 \times 1.2\text{m}$ dishes on a single platform. This array configuration yields a synthesized beam of FWHM $\simeq 2'$ ($0.6h^{-1}\text{Mpc}$ at $z = 0.8$), which is optimized to detect high-redshift clusters. The field-of-view of the primary beam is about $10'$. To generate the mock AMiBA visibility data, we perform a mosaic survey of 9×9 pointings with each exposure of $t_{\text{exp}} = 1.5$ hours covering 1deg^2 with spacing of 4.5 . The AMiBA sensitivity is then given as $\sigma_{\text{noise}}^S = 0.78(c_{\text{mos}}/0.83)(\eta/0.6)^{-1}(T_{\text{sys}}/70\text{K})(n_{\text{pol}}/2)^{-1/2}(B/20\text{GHz})^{-1/2}(t_{\text{exp}}/1.5\text{hours})^{-1/2}$ mJy/beam, where c_{mos} depends on the mosaicking strategy. The non-linear maximum entropy method is applied to reconstruct an AMiBA SZE map from the mock visibility data. For a weak lensing survey, we assume moderately deep optical observations with a mean source number density of $\bar{n} = 30\text{arcmin}^{-2}$ and $z_s = 1$. We take into account noise in observable image ellipticities due to the random-phase intrinsic source ellipticities. We choose the intrinsic dispersion of $\sigma_{\text{int}} = 0.4$. We then apply a pixelization on the mock weak lensing data using a Gaussian filter with FWHM = $2'$, and perform a linear mass inversion to reconstruct the κ -map. The sensitivity in reconstructed κ -maps is given as $\sigma_{\text{noise}}^\kappa = 1.75 \times 10^{-2}(\sigma_{\text{int}}/0.4)(\bar{n}/30\text{arcmin}^{-2})^{-1/2}(\text{FWHM}/2')^{-1}$. We carry out the statistical analysis on reconstructed sky maps by using the inner $41' \times 41'\text{arcmin}^2$ subfield in order to avoid the noisier boundaries. Thus the effective survey area used for our statistical analysis is $36 \times 0.47\text{deg}^2 \sim 17\text{deg}^2$.

3. Results

Figure 1 shows the theoretical halo number counts $N(> \nu)$ and false positive rate as a function of peak threshold $\nu (= S/\sigma_{\text{noise}}^S, \kappa/\sigma_{\text{noise}}^\kappa)$ obtained from mock AMiBA SZE and weak lensing surveys. To quantify the spurious peak detections due to experimental noise, we followed the prescription given by Ref. 5. The limiting halo masses $M_{\text{lim}}(z)$ for both surveys are shown in Figure 2. For both surveys, halo samples are defined at a false positive rate of 10%, and the redshift distributions of the halo samples are derived (see Figure 2). Further, we utilize the conditional number counts of weak lensing halos with faint SZE detection, $N(\kappa > \kappa_{\text{lim}} | S > S_{\text{lim}})$, to explore the potential of a combined AMiBA SZE and weak lensing survey. Here we choose the SZE peak threshold of $S_{\text{lim}} = 2.5\sigma_{\text{noise}}^S = 2\text{mJy/beam}$ (see Figure 1). Table 1 summarizes the main properties of halos samples obtained from mock AMiBA SZE and weak lensing observations.

4. Conclusions

We have examined the expected cluster number counts and redshift distributions of cluster samples for the forthcoming AMiBA SZE/weak lensing cluster survey on the basis of Λ CDM cosmological simulations. By utilizing the conditional halo number counts $N(\kappa > \kappa_{\text{lim}} | S > S_{\text{lim}})$, we have demonstrated that a combined SZE and weak lensing survey can gain an additional fainter halo sample at a given false positive rate, which cannot be obtained from either survey alone.

Acknowledgments

We would like to thank Mark Birkinshaw for fruitful discussions. AMiBA is funded by the Ministry of Education and National Science Council in Taiwan.

References

1. M. Birkinshaw, *Phys. Rep.*, **310**, 97 (1999).
2. M. Bartelmann and P. Schneider, *Astron. Astrophys.*, **345**, 17
3. K. Y. Lo, T. Chiueh, H. Liang, C.-P. Ma, R. N. Martin, K.-W. Ng, U.-L. Pen, and R. Subramanyan, in *IAU Symp. 201, New Cosmological Data and the Values of the Fundamental Parameters*, ed. A. Lasenby and A. Wilkinson (San Francisco: ASP), 31 (2000).
4. K.-Y. Lin, L. Lin, T.-P. Woo, Y.-H. Tseng, and T. Chiueh, *astro-ph/0210323*
5. P. Zhang, U.-L. Pen, and B. Wang, *Astrophys. J.*, **577**, 555

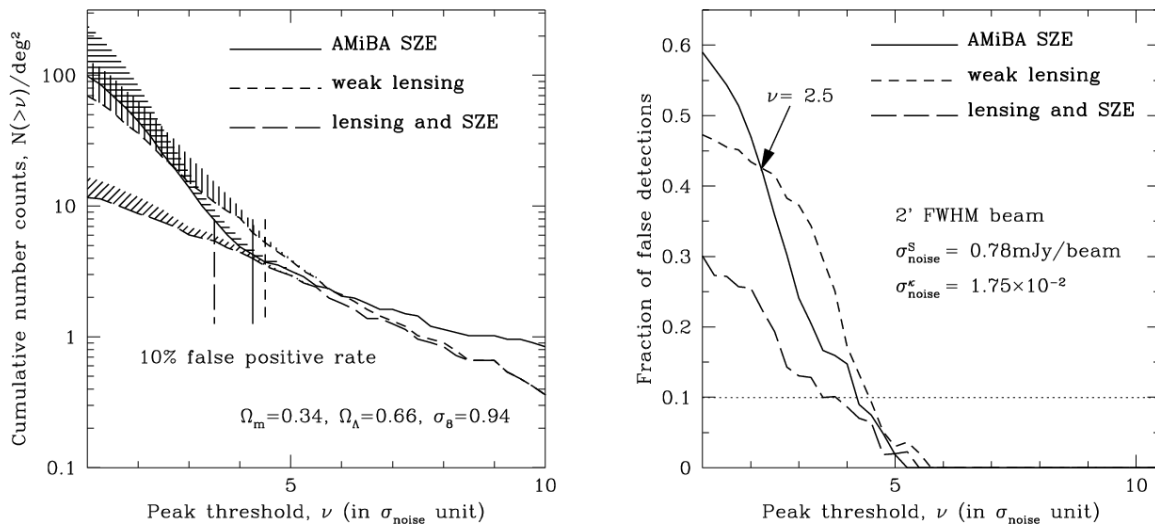
4 *Umetsu et al.*


Fig. 1. Left: Cumulative distribution functions $N(>\nu)$ of halo number counts in mock AMiBA (solid) and weak lensing (dashed) observations as a function of peak threshold $\nu(=S/\sigma_{\text{noise}}^S, \kappa/\sigma_{\text{noise}}^\kappa)$ derived from 36 simulated sky maps (17deg^2). The long-dashed curve represents the conditional number counts of weak lensing halos with faint SZE detection of $S > 2.5\sigma_{\text{noise}}^S = 2\text{mJy/beam}$. The shaded regions indicate false positive detections due to noise. Right: fraction of false detections as a function of peak threshold.

Simulation of a combined SZE and weak lensing cluster survey for AMiBA experiment 5

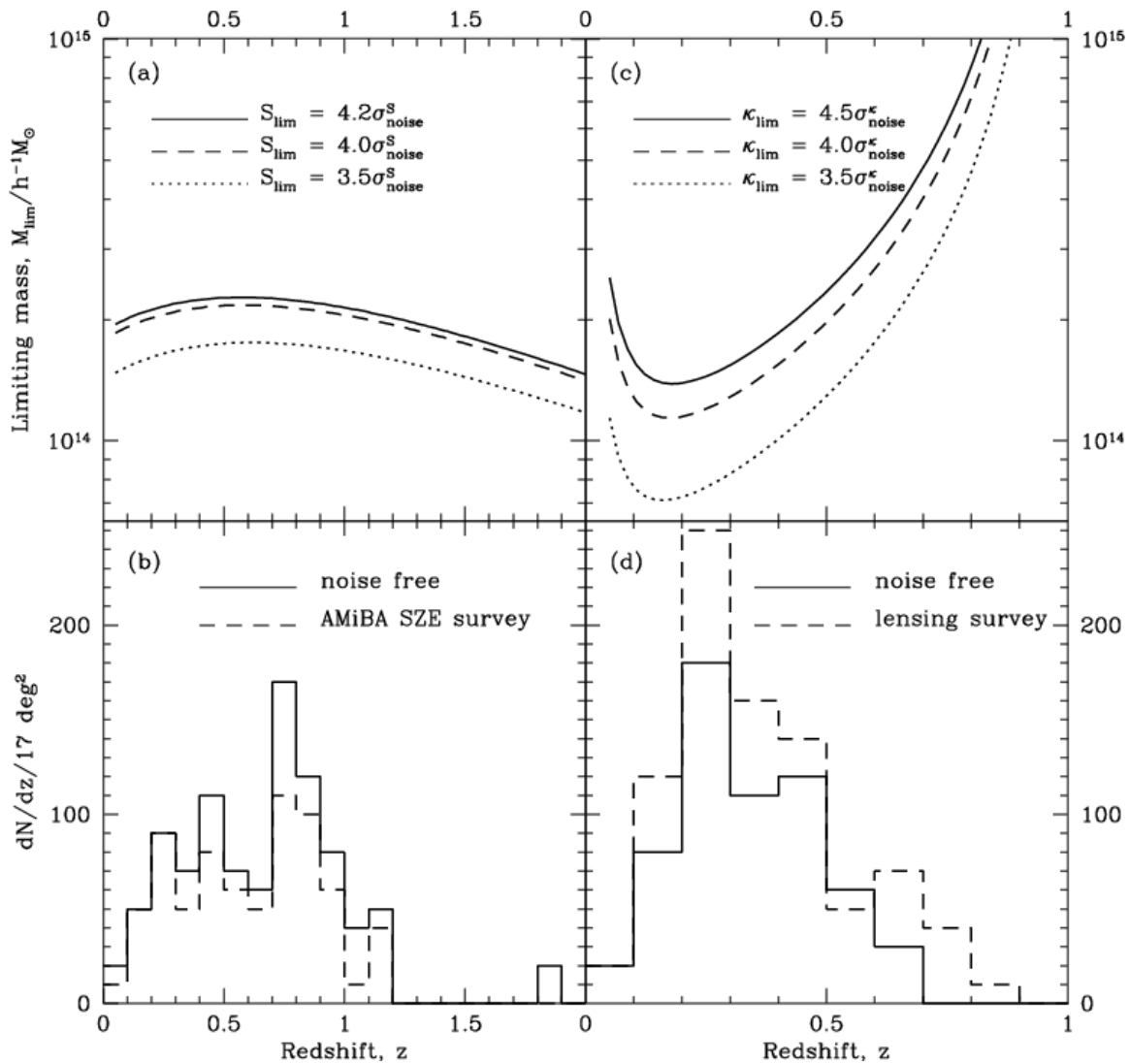


Fig. 2. Top: the limiting mass M_{lim} of halos as a function of redshift z for (a) AMiBA SZE and (c) weak lensing surveys (see Section 2). $M_{\text{lim}}(z)$ is calculated for three different peak thresholds. The solid curves correspond to a false positive rate of 10%. Bottom: redshift distributions of halo samples selected from mock 17deg^2 (b) AMiBA SZE and (d) weak lensing surveys.

6 *Umetsu et al.*

Table 1. Halo samples selected from mock AMiBA SZE and weak lensing surveys

Halo sample	limiting peak-flux S $\nu = S/\sigma_{\text{noise}}^S$	limiting peak κ -value $\nu = \kappa/\sigma_{\text{noise}}^\kappa$	N (deg $^{-2}$)
AMiBA SZE	$\nu > 4.2$		4.2
weak lensing		$\nu > 4.5$	5.2
combined AMiBA/lensing	$\nu > 2.5$	$\nu > 3.5$	4.9
faint	$2.5 < \nu < 4.2$	$3.5 < \nu < 4.5$	1.4